European Biophysics Journal, March 2013, Volume 42, Issue 2-3, pp 147-158

http://link.springer.com/article/10.1007/s00249-012-0871-z

Estimating the Rotation Rate in the Vacuolar Proton-ATPase in Native Yeast Vacuolar Membranes

Running Title: Rotation in V-ATPase

Csilla Ferencz[a], Pál Petrovszki[a], Zoltán Kóta[a], Elfrieda Fodor-Ayaydin[a,e], Lajos Haracska[b], Attila Bóta[c], Zoltán Varga[c], András Dér[a], Derek Marsh[d] and Tibor Páli[a,*]

[a]Institute of Biophysics, Biological Research Centre,
Temesvári krt. 62, 6726 Szeged, Hungary
Phone: +36-62-599603, FAX: +36-62-433133

[b]Institute of Genetics, Biological Research Centre,
Temesvári krt. 62, 6726 Szeged, Hungary

[c]Department of Biological Nanochemistry, Chemical Research Centre,
Pusztaszeri u. 59-67, H-1025 Budapest, Hungary

[d]Department of Spectroscopy, Max Planck Institute for Biophysical Chemistry,
Am Fassberg 11, 37077 Göttingen, Germany

[e]Present address: Institute of Biochemistry, Biological Research Centre,
Temesvári krt. 62, 6726 Szeged, Hungary

* To whom correspondence should be addressed. E-mail: tpali@brc.hu .

Abstract

The rate of rotation of the rotor of the yeast vacuolar proton-ATPase (V-ATPase), relative to the stator or the steady parts of enzyme, is estimated in native vacuolar membrane vesicles of Saccharomyces cerevisiae under standardised conditions. Membrane vesicles are spontaneously formed after exposing purified yeast vacuoles to osmotic shock. The fraction of the total ATPase activity originating from V-ATPase is determined using the potent and specific inhibitor of the enzyme, concanamycin A. Inorganic phosphate liberated from ATP in the vacuolar membrane vesicle system, during 10 min of ATPase activity at 20 °C, is assayed spectrophotometrically for different concanamycin A concentrations. A fit to the quadratic binding equation, assuming a single concanamycin A binding site on a monomeric V-ATPase (our data is incompatible with models assuming more binding sites) to the inhibitor titration curve determines the concentration of the enzyme. Combining it with the known rotation:ATP stoichiometry of V-ATPase and the assayed concentration of inorganic phosphate liberated by V-ATPase leads to an average rate of ~9.53 Hz of the 360 degrees rotation, which, according to the time-dependence of the activity, extrapolates to ~14.14 Hz for the beginning of the reaction. These are low limit estimates. To our knowledge this is the first report of the rotation rate in a V-ATPase that is not subjected to genetic or chemical modification and it is not fixed on a solid support, instead it is functioning in its native membrane environment.

Special Issue: Structure, function, folding and assembly of membrane proteins — Insight from Biophysics.

Key Words: ATP synthase • ATPase • concanamycin • F-ATPase • native membrane • rotary enzyme • vacuolar proton-ATPase • vacuole • V-ATPase • yeast

Introduction

The proton-translocating adenosine-triphosphatase (first observed in vacuolar membranes, hence called vacuolar proton-ATPase or V-ATPase) is nature's most universal proton pump found in all eukaryots (Finbow and Harrison 1997; Nishi and Forgac 2002; Cipriano et al. 2008; Jefferies et al. 2008). Similarly to the more familiar and related F-ATP synthase (F-ATPase) there are 3 catalytic sites, here for ATP hydrolysis, in the water soluble V_1 domain (F_1 domain in F-ATPase), and trans-membrane proton transport takes places in hydrophilic channels (or sacks) in the interface between the "c ring" and subunit a of the membrane bound V_o (F_o) domain (Wilkens et al. 1999; Grabe et al. 2000; Kawasaki-Nishi et al. 2001; Kawasaki-Nishi et al. 2001; Wang et al. 2004; Beyenbach and Wieczorek 2006) (Fig. 1). Crucial for proton transport are the unique glutamic acid residues, one on each subunit c: binding, e.g., dicyclohexyl-carbodiimide to this glutamic acid blocks both proton transport and ATP hydrolysis (Linnett and Beechey 1979; Wada et al. 2000; Perez-Sayans et al. 2009), proving that catalysis and transport are strongly coupled (Futai et al. 2000; Kawasaki-Nishi et al. 2001). In both enzymes this coupling involves a rotation of the rotor relative to the rest of the protein that can be considered as the stator (Yasuda et al. 1997; Fillingame et al. 2000; Futai et al. 2000; Yasuda et al. 2001; Rondelez et al. 2005; Ueno et al. 2005). The rotor vs. stator subunits of V-ATPase are not the same as those of the V_o vs. V_1 domains, since subunits a and d of V_o belong to the stator, and subunits D and F of V_1 belong to the rotor (other subunits of V_o and V_1 belong to the rotor and stator, respectively) (Ubbink-Kok et al. 2000).

Rotation is needed to bring protons, bound to the protonated glutamic acid, from the input channel to the output channel through the hydrophobic interface between the lipid matrix and the c ring (Fig. 1). In the case of V-ATPase rotation is driven by ATP binding and hydrolysis. One ATP molecule drives a 120 degrees rotation of the rotor and a transport of two protons from the cytoplasmic side to the "other" side, which can be the lumen of intracellular organs or the extracellular space, depending on the cellular location of V-ATPase (Finbow and Harrison 1997; Nishi and Forgac 2002; Beyenbach and Wieczorek 2006; Cipriano et al. 2008; Jefferies et al. 2008). This stoichiomerty is different form that of F-ATPase, in which there are ~12 c subunits, which have only 2 trans-membrane helices, each with a unique glutamic acid. So in F-ATPase a synthesis of one ATP also drives 120 degrees rotation, which, however, requires a movement of 4 subunits c, hence 4 protons (Van Walraven et al. 1996; Panke and Rumberg 1997; Stock et al. 1999; Ferguson 2000; Seelert et al. 2000; Stahlberg et al. 2001). In the case of F-ATPase rotation and ATP synthesis is driven by trans-membrane delta pH, but it should be noted that both enzymes can work in both directions depending on the conditions (Yoshida et al. 2001; Itoh et al. 2004; Rondelez et al. 2005; Feniouk et al. 2007; Nakano et al. 2008). Another difference between these related rotary engines is that whereas the c ring of the F-ATPase is built from identical c subunits, each having two trans-membrane alpha helices (Dmitriev et al. 1999; Fillingame et al. 2000), the c ring in V-ATPase consist of 4 c subunits and one copies of c' and c" subunits each (Hirata et al. 1997; Powell et al. 2000). The reason for this heteroge-

neity is not known but it might have to do with the regulation of V-ATPase and the fact that c ring appears in different tissues in roles as, e.g., gap junctional and neurotransmitter release channels, or parts of membrane fusion machineries, not related to V-ATPase (Holzenburg et al. 1993; Baars et al. 2007; El Far and Seagar 2011; Strasser et al. 2011). In addition, subunit c" has 5 transmembrane helices (Hirata et al. 1997; Gibson et al. 2002). Nevertheless, despite the size difference between the subunit c of the F_o and V_o, the first and second two trans-membrane helices of the V-ATPase are highly homologous to each other (but the unique glutamic acid is only present on helix 4) and to subunit c of the F-ATPase. Indeed, these and other highly homologous proteins belong to the same class, that we termed ductins (Finbow et al. 1994; Dunlop et al. 1995; Finbow et al. 1995; Saito et al. 1998; Bohrmann and Bonafede 2001). In a number studies on a 16kDa gap junctional protein isolated from lobster, which is not only a ductin protein but it can substitute subunit c of the yeast V-ATPase functionally in a hybrid construct (Finbow et al. 1993; Finbow and Harrison 1997), we have shown that the c ring is a hexameric assembly of 4-helix trans-membrane bundles (Holzenburg et al. 1993; Pali et al. 1995), determined the vertical membrane location of the unique glutamic acid and shown it to contact lipids (Pali et al. 1997; Pali et al. 1999), and discovered a metal binding site (Pali et al. 2006).

Specific inhibitors of V-ATPase are important because the enzyme is a potential therapeutic target in certain diseases, e.g., osteoporosis, deafness and cancer (Linnett and Beechey 1979; Farina and Gagliardi 1999; Bowman and Bowman 2005; Lu et al. 2005; Morimura et al. 2008; Otero-Rey et al. 2008; Supino et al. 2008; Hinton et al. 2009; Perez-Sayans et al. 2009; McHenry et al. 2010; Nishisho et al. 2011). The macrolide antibiotics concanamycin A and bafilomycin are the most potent and most selective inhibitors of V-ATPase, with IC_{50} values down to the nM region (Bowman et al. 1988; Farina and Gagliardi 1999; Gagliardi et al. 1999; Huss et al. 2002; Dixon et al. 2008). We have demonstrated recently that concanamycin A and its synthetic indole analogues (Dixon et al. 2003) incorporate readily into membranes (Dixon et al. 2004; Pali et al. 2004) and interact with amino acid side chains of the 16kDa lobster (Nephrops norvegicus) protein and also with subunit c of yeast V-ATPase (Pali et al. 2004; Dixon et al. 2008). It was not subject of those studies to probe interaction of the inhibitors with subunits c', c" and a of the yeast V-ATPase, but they do interact with polypeptides based on sequences of the putative interfacial trans-membrane helices of these subunits (Kota et al. 2008). The inhibitors have also been shown to perturb the lipid-protein interface around the c ring (Pali et al. 2004).

The most logical question with respect to the rotary mechanism, namely what is the rate of rotation of the rotor, is a most difficult one to answer, because it can only be measured directly only if the enzyme is modified to a great extent. All direct measurements (see (Nakanishi-Matsui et al. 2010) for a recent review), both on V- and F-ATPase, rely on gene-engineered modification of the enzyme in order to do single molecule fluorescence resonance energy transfer experiments, or, more commonly attach a visualisation elements, e.g., fluorescent filament or polystyrene or gold bead, to the rotor (or stator) and fix the stator (or rotor) on a solid support, followed by visualisation of the rotation (Noji et al. 1997; Tsunoda et al. 2001; Nishio et al. 2002; Hirata et al. 2003; Nakanishi-Matsui et al. 2006; Xie 2009; Sekiya et al. 2010; Furuike

et al. 2011; Kohori et al. 2011; Okuno et al. 2011). Such modifications may add or remove barriers to the rotation not present in the native system. Consequently, the reported rotation rates vary greatly in such studies, depending on the gene-engineered construct and the details of the artificial environment of the enzyme (Panke and Rumberg 1997; Masaike et al. 2000; Itoh et al. 2004; Imamura et al. 2005; Adachi et al. 2007; Takeda et al. 2009). Such studies are not possible on a native enzyme in a native membrane, but since the ATP/rotation stoichiometry is known, one could assay the inorganic phosphate liberated from ATP hydrolysis by V-ATPase in unit time and relate it to the concentration of V-ATPase. However, reliable estimates on the rotation in native V-ATPase in a native membrane are still lacking because of several problems with this approach: (i) how to separate the activity of V-ATPase from other ATPases, (ii) how to determine its concentration, (iii) how to determine the fraction of inactive V-ATPases? (In some cases there are as much as ten-fold differences reported by direct and indirect methods, based on activity measurements on the F-ATPase, even in the very same artificial system, in which the enzyme concentration is known. This discrepancy was attributed to the fraction of as high as 90% inactive F-ATPases (Yasuda et al. 2001; Ueno et al. 2005; Nakanishi-Matsui et al. 2006; Sekiya et al. 2009; Nakanishi-Matsui et al. 2010; Furuike et al. 2011).

In the present study ATPase activity in yeast vacuolar membrane vesicles was measured. The activity of V-ATPase from other ATPases was separated with the help of the specific V-ATPase inhibitor concanamycin A. Typically about 60% of the total activity comes from V-ATPase in our system. The conditions were standardised and the absorbance was calibrated for phosphate liberated in unit time. The concentration of the enzyme was determined from the inhibitor titration experiment, fitted with a model of one inhibitor binding site per V-ATPase. Combination of the data yields a rate of 9.53 Hz for the 360 degrees rotation of the rotor, hence the complete catalytic cycle. This is a low limit estimate, considering the probably less than 100% activity of the inhibitor and V-ATPases (even in the absence of inhibitor).

Materials and Methods

Materials

The lyticase enzyme (crude, from Arthrobacter luteus), concanamycin A, bafilomycin, ascorbic acid, sodium dodecyl sulphate (SDS), DL-Dithiothreitol (DTT), sodium orthovanadate (Na_3VO_4), 2-(N-Morpholino)ethanesulfonic acid hydrate (MES) were purchased from Fluka (Sigma), Na_2ATP (adenosine 5′-triphosphate disodium salt hydrate) from Serva, ficoll from Fluka. D(-)-sorbitol, yeast extract, glucose and peptone were purchased from Molar, Tris(hydroxymethyl)aminomethane (TRIS), sodium azide (NaN_3), ammonium molybdate tetrahydrate form Reanal (Hungary). All standard chemicals were of analytical grade purity.

Yeast cell culture

Cells (Saccharomyces cerevisiae EMY 74.7) were grown in YPD medium (2% glucose, 2% peptone and 1% yeast extract) at 30 °C in a water bath shaker (New Brunswick Scientific Co. Inc.) with consistent agitation. For vacuolar membrane vesicles isolation, overnight cultures were diluted to OD_{600} = 0.1 in 1 L YPD media, and cells were harvested when cultures reached OD_{600} = 0.8-1.

Isolation of vacuoles and preparation of vacuolar vesicles

Preparation of yeast vacuolar membrane vesicles were based on (Ohsumi et al. 1983; Uchida et al. 1985) with some modifications. Briefly, exponentially growing cells were harvested by centrifugation at 5400 rpm for 30 min at 4 °C. The pellet was resuspended in TRIS buffer (100 mM TRIS, 10 mM DTT, 10 mM NaN_3, pH 9.4) and centrifuged in a SS-34 rotor (Sorvall rotors were used in a Sorvall RC-5C centrifuge unless stated otherwise) at 6500 rpm for 5 min at 4 °C. The pellet was resuspended in spheroplast buffer (1.5 M sorbitol, 50 mM TRIS, 2 mM $MgCl_2$, 10 mM NaN_3, pH 7.2), which was supplemented with lyticase to a final concentration of 1 unit/mL. The suspension was incubated at 30 °C for 90 min, during gentle shaking. Spheroplasts were cooled on ice and layered on the top of 5 ml 1.9 M sorbitol and centrifuged in a HB-4 rotor at 2100 rpm for 5 min at 4 °C. The so recovered spheroplasts were washed by centrifugation (3800 rpm, 5 min at 4 °C) with 1 M sorbitol. The pellet was re-suspended in buffer A (10 mM MES/TRIS, 0.1 mM $MgCl_2$, 12% Ficoll-400, pH 6.9) supplemented with protease inhibitor cocktail tablet (Roche). The resulting mixture was then homogenised by a Dounce homogenizer with 30 strokes and centrifuged at 5200 rpm for 5 min at 4 °C. For the isolation of vacuoles 5 ml of the supernatant was transferred into an ultracentrifuge tube, 5 ml of buffer A was gently layered on the top, and centrifuged in TH-641 rotor at 12500 rpm for 30 min at 4 °C (in a Sorvall Discovery 90SE ultracentrifuge by Hitachi). Vacuoles, the white layer

on the top, were recovered. Vacuolar membrane vesicles were formed following osmotic shock by diluting the vacuole suspension ten-fold with buffer C (10 mM MES/TRIS, 5 mM $MgCl_2$, 25 mM KCl, pH 6.9) and gently shaking up the pellet. The vesicle suspension was centrifuged in AH-627 rotor at 15000 rpm for 30 min at 4 °C in the same centrifuge. The vesicles were collected as the pellet in the same buffer. The total protein content was determined according to (Lowry et al. 1951) and the vesicles were stored at -80 °C in buffer C and 10% glycerol.

Light microscopy of yeast vacuoles

Transmitted light mode microscopy images of the vacuole suspensions were observed using differential interference contrast optics of Olympus IX81 inverted microscope. Images were captured with F-View 12-bit monochrome CCD camera using Olympus Cell-R software and UPlanSApo 60x oil immersion objective with a numerical aperture of 1.35.

Freeze-fracture electron microscopy of vacuolar membrane vesicles

Freeze-fracture electron microscopy was used for direct visualisation of the membrane structures evolved from the vacuoles. Glycerol was added to the vesicle dispersion as cryoprotectant at a final concentration of 20 %. Addition of glycerol does not alter the bilayer structure, but inhibits the aggregation and ice crystal damage of the vesicles during the freezing process @<should come a ref. form Zoltan Varga>@. The gold sample holders used in freeze fracture were pre-incubated at 24 °C at the same temperatures as the samples. Droplets of 1-2 µL of the sample were pipetted onto a gold sample holder and frozen by plunging it immediately into partially solidified Freon for 20 s and stored in liquid nitrogen. Fracturing was performed at -100 °C in a Balzers freeze-fracture device (Balzers BAF 400D, Balzers AG, Vaduz, Liechtenstein). The replicas of the fractured faces etched at -100 °C for 30 s were made by platinum-carbon shadowing then cleaned with a water solution of surfactant and washed with distilled water. The replicas were placed on 200 mesh copper grids and examined in a Morgani 268D (FEI, Eindhoven, the Netherlands) transmission electron microscope.

ATPase activity assay

Vesicle suspension of 10 µg of total protein was used to assay ATPase activity in 250 µl of assay mixture. Our activity assay and the use of inhibitors was based on (Serrano 1978; Clelland and Saleuddin 2000; Lunde and Kubo 2000; Padilla-Lopez and Pearce 2006), with modifications, as follows. The assay mixture contained the activity buffer (50 mM MES/TRIS, 5 mM $MgCl_2$, pH 7.0), 5 mM sodium azide (to inhibit mitochondrial ATPase), 0.2 mM ammonium molybdate (to inhibit acid phosphatases), 100 µM sodium orthovanadate (to inhibit plasma membrane proton-ATPase). In some of the substrate titration experiments (Fig. 4) the $MgCl_2$ concentration was adjusted twice to that of Na_2ATP. Except for the inhibitor titration experi-

ment (Fig. 6), the final concentration of the specific V-ATPase inhibitor concanamycin A was 1 μM. Vacuolar vesicles were incubated in the activity buffer at room temperatures for 30 min. ATP hydrolysis was started by adding 2 mM Na_2ATP and was going on at 30 °C for 20 min, except that it was 10 min in the inhibitor titration experiment (Fig. 6) and it was varied in the time dependence (Fig. 5). The reaction was stopped with a solution containing 0.5% SDS, 2% H_2SO_4, 0.5% ammonium molybdate tetrahydrate and 10% ascorbic acid. The acid was added to start the colour development of the reaction due to inorganic phosphate production, a product of ATP hydrolysis. The vesicle suspension was incubated in this stopping buffer at room temperature for 20 min. Absorbance was measured at 750 nm in a Thermo Spectronic (USA) spectrophotometer. All data analysis and curve fitting was done with the IGOR scientific graphing and data analysis program (WaveMetrics, Lake Oswego).

Results and discussion

Fig. 2A shows a typical bright field transmitted light microscopy image of intact vacuoles as we purified them from yeast Saccharomyces cerevisiae. We did not use vacuoles for activity measurements because (i) the ATPase activity originating from other ATPases is rather high in comparison to that of V-ATPase (data not shown), (ii) these vacuoles were rather unstable and (iii) the osmotic conditions needed to keep the vacuoles intact were not optimal for administering other compounds, in general for washing, and for the activity assays. Therefore, it was decided to wash the vacuoles and let the osmotic shock break them. Interestingly, simply this step alone led to the spontaneous formation of vesicles from vacuolar membrane fragments. Fig. 2B shows a typical freeze-fracture electron microscopic image of such vesicles. This vesicular system turned out to be rather stable, as it tolerated storage up to 10 weeks (not tested longer) at −80 oC @<Pali: how long was the longest storage?>@. In addition, and most importantly, this step allowed us to wash away most of the water-soluble ATPases from the suspension, maximising the relative contribution of V-ATPase to the total ATPase activity of the sample, as proven in Fig. 3, which shows ATPase activities of yeast vacuolar vesicles in the presence and absence of different ATPase inhibitors. In this experiment, the concentration of inorganic phosphate was assayed after 20 min of incubation of the vacuolar vesicles at 30 °C in the presence of 2 mM Na_2ATP and 5 mM $MgCl_2$ (except for the first two bars). Since the substrate of the reaction is MgATP and $MgCl_2$ is in excess to Na_2ATP, the substrate concentration was close to 2 mM (at least in the beginning of the reaction). Several inhibitors that are known to inhibit other ATPases (Serrano 1978; Clelland and Saleuddin 2000; Lunde and Kubo 2000; Padilla-Lopez and Pearce 2006) were tested. These 'other' inhibitors removed only about 20% of the total ATPase activity, even at relatively high inhibitor concentration. Di-cyclohexyl-carbodiimide, which inhibits proton translocation also in the related F-ATPase (see, e.g., (Kopecky et al. 1981; Kopecky et al. 1982; Kopecky et al. 1983; Hermolin and Fillingame 1989; Wada et al. 2000)), was more potent, but the most potent inhibitors were, as expected, concanamycin A and bafilomycin, even when applied at the lowest concentrations (Bowman et al. 1988; Drose et al. 1993; Gagliardi et al. 1999; Huss et al. 2002; Dixon et al. 2008). In this system, and under the present conditions, these inhibitors removed ~60% of the total ATPase activity, which varied to some extent from isolation to isolation. Since these two inhibitors are known to be very potent and very selective inhibitors of V-ATPase (Bowman et al. 1988; Farina and Gagliardi 1999; Huss et al. 2002; Dixon et al. 2008) ~60% of the total ATPase activity comes from V-ATPase in these vesicular preparations.

In order to standardise the conditions for the activity measurements the optimal substrate concentration has to be determined. This has been done by measuring the absorbances (at 750 nm) of inorganic phosphate liberated by ATP hydrolysis in the vacuolar vesicles, and assayed after 20 min incubation at 30 °C, as a function of the concentration of exogenously added Na_2ATP, both at fixed (5 mM) $MgCl_2$ concentration (circles) or when it was set to 2-fold that of the Na_2ATP (squares). Fig. 4 shows the concentration dependence of the whole system (no in-

hibitor, white symbols) and that of V-ATPase alone (black symbols). The latter one is obtained as the difference in absorbance ± (1 μM) concanamycin A. The data are normalised such that the maximum activity is the same, i.e., unity, in the absence of the inhibitor. The whole system saturates at ~2 and ~10 mM Na_2ATP, in the excess and fixed $MgCl_2$ concentration case, respectively, and the production of inorganic phosphate decreases at high substrate concentrations (only measured for the latter case). The reason for the downward shift of the saturation lies most probably in the different ATP/Mg stoichiometries in the two cases. This, however, does not influence the point of maximum activity of V-ATPase (= 2 − 3 mM Na_2ATP) because at that concentration even 5 mM $MgCl_2$ can be considered as in excess. Note that 2 mM substrate is considered as high ATP or full speed condition (see, e.g., (Noji et al. 1997; Yasuda et al. 1997; Yasuda et al. 2001; Ueno et al. 2005; Furuike et al. 2011)). We don't know the exact reason of the drop of the activity, also in the case of V-ATPase, at higher substrate concentrations, but one can speculate that, due to the ATP ™ ADP + Pi dissociation and maybe even ADP impurities in the ATP stock, the ADP concentration might reach a level at which it significantly inhibits ATPases (De la Cruz et al. 2000; Nakano et al. 2008). Nevertheless, a choice of 2 mM Na_2ATP and 5 mM $MgCl_2$ ensures that this kind of inhibition is negligible, and that V-ATPase is running at highest speed with respect to substrate concentration, at least at the beginning of the incubation period, which also needs to be standardised in order to avoid consumption of all substrate during the reaction.

Fig. 5 shows the time-dependence of (delta) absorbances obtained as the difference between the absorbances of assayed inorganic phosphate liberated by ATP hydrolysis by yeast vacuolar vesicles in the absence and presence of 1 μM of the specific V-ATPase inhibitor concanamycin A, at 20 °C and in the presence of exogenously added 2 mM Na_2ATP and 5 mM $MgCl_2$. As shown above the absorbance difference of ± (1 μM) concanamycin A measures phosphate liberated exclusively by V-ATPase. Since the substrate concentration decreases during the reaction, the rate of ATP hydrolysis by V-ATPase decreases monotonically too. The semi-kinetic curve does not follow a single exponential, as demonstrated by the poorness of the single exponential fit over the whole incubation period. The reason is that the product, ADP, inhibits the enzyme (De la Cruz et al. 2000; Nakano et al. 2008). Obviously, the fit over the first 20 minutes, where the concentration of the product is much lower, is closer to a single exponential. It should be noted that the exponential fits are presented just for the visualisation and they were not used in this study for any further analysis. Based on this experiment, the duration of the reaction was chosen to be 10 min, as it is short enough to avoid significant consumption of the substrate but long enough to obtain a conveniently high yield of Pi liberated by V-ATPase. Comparing the $\Delta A/\Delta t$ slope of the fit to the first 5 points (onset slope) with the slope of the line connecting the points at 1 and 10 min (straight lines in Fig. 5), one can estimate the rate of ATP hydrolysis at the beginning of the incubation period if the mean is known. The ratio between the two slopes is 1.48.

Under the above standardised conditions, and including the spectrophotometric calibration for inorganic phosphate (Fig. 6, see below) and using the specific inhibitor concanamycin A, one can determine the concentration of ATP hydrolysed exclusively by V-ATPase in unit

time. The enzyme concentration, needed to convert this data into revolutions of the rotor per second can be determined from the experimental inhibitor titration curve (Fig. 6) fitted with the appropriate binding equation, because the concentration of the inhibitor is known and the shape of the curve depends (differently) on the enzyme concentration and the dissociation constant of the enzyme-inhibitor binding. The general case is presented below with n independent and identical inhibitor binding sites per enzyme, assuming non-cooperative binding. Further, it is assumed that all inhibitor molecules (I) are active and all V-ATPase molecules are active if no inhibitor is bound (it is considered later the case when these assumptions don't hold), but are inactivated when at least one inhibitor is bound. The data on Fig. 6 should follow the equation

$$A(I_t) = (A_0 - \Delta A) + \Delta A * P_f / P_t \,, \qquad [1]$$

where $A(I_t)$ is the absorbance considered as a function of the total inhibitor concentration, I_t. A_0 is the absorbance in the absence of inhibitor, a constant (3 measurements gave an average of 1.248). ΔA is the difference of the absorbances at zero and saturating concentration of the inhibitor. It could be determined experimentally but it is also a fitting parameter in the present study because the inhibitor concentration is not sufficiently high. P_t is the (total) enzyme concentration and P_f is the concentration of the enzyme without any inhibitor bound (the indices t, f, b mean all, free and bound sites or molecules, respectively, and the letters indexed with these mean concentrations). The relevant binding equations need to be solved to derive P_f / P_t as a function of I_t (the formalism is similar to that presented in, e.g., (Sandermann 1982)). If the binding sites (B) are equivalent and independent the binding reaction is

$$B + I \text{ ™ } BI \,,$$

where BI means occupied binding site, i.e., bound inhibitor. The corresponding binding equation is

$$B_f * I_f = I_b * K \,, \qquad [2]$$

where K is the dissociation constant of the inhibitor binding to an independent binding site. Since $B_f = n * P_t - I_b$ and $I_f = I_t - I_b$ it follows that

$$(n * P_t - I_b) * (I_t - I_b) = I_b * K \,. \qquad [3]$$

This quadratic equation can be solved for the concentration of the bound inhibitor:

$$I_b = (I_t + n * P_t + K - \mathrm{sqrt}((I_t + n * P_t + K)^2 - 4 * n * P_t * I_t)) / 2 \,. \qquad [4]$$

If there is only a single binding site per enzyme (n = 1), then $B_f = P_f = P_t - I_b$, and therefore

$$P_f / P_t = (P_t - I_b) / P_t = (P_t - I_t - K + \mathrm{sqrt}((I_t + P_t + K)^2 - 4 * P_t * I_t)) / (2 * Pt). \qquad [5]$$

Substituting the right side of Eq. [5], with n = 1, in place of P_f / P_t in Eq. [1] yields the function suitable for fitting the data in Fig. 6 with the single binding site model:

$$A(I_t) = (A_0 - \Delta A) + \Delta A * (P_t - I_t - K + \mathrm{sqrt}((I_t + P_t + K)^2 - 4 * P_t * I_t)) / (2 * Pt) \,. \qquad [6]$$

In these fits I_t is the independent variable and P_t, K and ΔA are fitting parameters.

Let us now consider the binding stoichiometries and reaction at the level of the enzyme with n binding sites:

$$P0 + I \text{ ™ } PI_1 \text{ , } PI_1 + I \text{ ™ } PI_2 \text{ , } \ldots PI_{n-1} + I \text{ ™ } PI_n \text{ ,}$$

where P0 is the enzyme without any inhibitor bound. PI_i represents the enzyme with i inhibitors bound (i = 1, 2, … n) and P_i is its concentration, so $P_f = P_0$. Considering the free and occupied binding sites in the above reactants and the transport balance of the inhibitors, one can write the binding equations for the corresponding concentrations in a generalised recursive form as

$$I_f * P_{i-1} * f_{on} * (n + 1 - i) = P_i * f_{off} * i \text{ , with } i = 1, 2, \ldots n \text{ ,}$$

Where f_{on} and f_{off} are the intrinsic on and off rates, respectively. The factor (n + 1 - i) is the number free binding sites on PI_{i-1} and i is the number of the occupied (bound) sites on PI_i. The intrinsic dissociation constant is $K = f_{off} / f_{on}$, and since $I_f = I_t - I_b$, we define $I_k = (I_t - I_b) / K$, and the recursive form simplifies to

$$P_i = P_{i-1} * I_k * (n +1 - i) / i \text{ , with } i = 1, 2, \ldots n \text{ .} \qquad [7]$$

Since $P_t = P_0 + P_1 + P_2 \ldots + P_n$, this leads to the polynomial expansion and therefore the closed form of the result is

$$P_f / P_t = P_0 / P_t = 1 / (1 + I_k)^n \text{ .} \qquad [8]$$

Note that if n = 1 Eq. [8] simplifies to

$$1 / (1 + P_1 / P_f) = 1 / (1 + I_f / K) \text{ from which } P_1 / P_f = I_f / K \text{ ,}$$

and since in this case $P_1 = I_b$ this expression is identical with Eq. [3] (with n = 1), i.e., it correctly reduces back to the single binding site situation above. Combining Eq. [8] with Eq. [1] leads to a function that is suitable for fitting the experimental data in Fig 6 with the multiple binding site model, such as

$$A(I_t) = (A_0 - \Delta A) + \Delta A * (1 + I_k)^{-n} \text{ .} \qquad [9]$$

(One needs to substitute the definition of I_k and I_b (from Eq. [4]) into Eq. [9] for the complete expression.) The fitting parameters are the same as in the case of n = 1 (Eq. [6]).

A fit to Eq. 9, where all parameters are released (not shown), including the number of binding sites n, yields n = 0.75 ± 0.58. Since non-integer number of binding sites on a monomeric enzyme is impossible, and there is no reason to assume a binding of 3 inhibitors to 4 enzymes, one can fix n = 1, i.e., settle on the single binding site situation. Indeed, as a test, neither the n = 2 nor the n = 5 model gives a better fit (n > 5 would not make sense because no more than 5 c ring subunits are available for binding). In fact, the fits with these models yield physically impossible parameters, e.g., negative enzyme concentration (P_t), even if some of the pa-

rameters (ΔA or K) are fixed at their values from the above fit with n = 1. To illustrate this, Fig. 6 also shows the best fit with n = 5 (dotted line) when, however, P_t is fixed at the value from the fit to n = 1 model. Obviously, ΔA is wrong and the fit is much worse than that with n = 1. One can conclude that our data is only compatible with the single binding site, n = 1 model. The fit with this model (solid curve in Fig. 6) yields the following results when all parameters are released (except that n = 1 is fixed): P_t = 44.9 ± 31.6 nM, K = 49.26 ± 18.2 nM, ΔA = 0.871 ± 0.023 (errors are ± standard errors from the fit). If ΔA (the most accurate fitting parameter) is then fixed at 0.871 the other parameters do not change but their standard deviation become smaller: P_t = 44.9 ± 24.6 nM and K = 49.25 ± 11.5 nM. The absolute amount of inorganic phosphate corresponding to ΔA is liberated exclusively by 44.90 ± 24.6 nM V-ATPase. The inset in Fig. 6 shows the phosphate calibration in the very same system. The slope of the linear regression is 0.00452 OD/nmole Pi, with which the concentration of Pi liberated by V-ATPase is 769.96 μM. Taking the ratios of the mean concentrations one concludes that in 10 min 17149.5 Pi molecules, i.e., 28.58 per second, were liberated by each V-ATPase molecules. Current understanding of the V-ATPase catalysis assume a hydrolysis of 3 ATP molecules in a complete 360 degrees rotation cycle (see., e.g., (Beyenbach and Wieczorek 2006)), which means that the rotation rate in V-ATPase in our vacuolar membrane vesicle system is 9.53 Hz at 20 °C and under excess ATP condition. If we consider the ± standard deviation of the fitting parameter P_t, i.e., the one with the largest relative fitting error, the range of rotation rates is 6.2 − 21.1 Hz. Comparing the slopes in the time dependence (Fig. 5) at the onset of the reaction and that connecting the 1-10 min points, the mean rotation rate extrapolates to ~14.14 Hz and to a range of rotation rates of 9.2 − 31.2 Hz, for the beginning of the reaction.

It should be noted that the dissociation constant, K, of concanamycin A binding to V-ATPase is much larger than in some early reports (Bowman et al. 1988; Drose et al. 1993) but similar to a more recent report (Whyteside et al. 2005; Dixon et al. 2008). In addition to the difference in the host systems, this discrepancy might be caused by several factors as explained in (Whyteside et al. 2005), of which, the most likely might be a potential removal of a structural component (e.g., polypeptide or lipid) required for a higher affinity binding. The state of the membrane might play a role here, since concanamycin A have been demonstrated to penetrate into the membrane and interact directly with both the lipids and side chains of subunits c (Pali et al. 2004; Pali et al. 2004; Dixon et al. 2008; Kota et al. 2008). There is no reason to assume that the composition and the concentration of the lipids changed significantly from preparation to preparation (the samples were taken to have the same mass of total protein) but the membrane environment of V-ATPase might be very different in different studies.

Conclusions

Reports on the rate of rotation in V-ATPase vary widely. One reason is that the enzyme is in a very different state and environment in activity measurements in native like membranes versus direct observations of the rotation of attached fluorescent or gold particles when it is fixed on a solid support. In some cases there are as large as ten fold differences between activity based estimates and direct observations even for the very same system (Nakanishi-Matsui et al. 2010). Such discrepancies are explained by the differences in the ratio of inactive/active V-ATPase, an unknown factor, in different systems. In view of the preparation to preparation variations and in comparison with other ATPases in the system (Fig. 2), we believe that so big variations in the inactive/active ratio are unlikely. The present approach, to use the inhibitor titration curve in order to determine the concentration of the enzyme and the dissociation constant of the inhibitor, depends on the chemistry of the inhibitor-V-ATPase interaction. Our data is compatible only with a single binding site per monomeric enzyme. Since concanamycin A most likely binds to intramembranous subunits (Pali et al. 2004; Pali et al. 2004; Whyteside et al. 2005; Bowman et al. 2006; Dixon et al. 2008), the present result suggests that an interaction with a single subunit c is not sufficient for concanamycin A binding: it either binds to more than one subunits or it binds to either subunit a, c' or c" (Huss et al. 2002), of which there are only one copies in the structure, although its interaction with the lobster c ring and other recent data (Pali et al. 2004; Bowman et al. 2006; Dixon et al. 2008) argue against c' and c'' being the binding sites. The accuracy of our approach could be further improved by adding more points to the inhibitor titration curve. However, it would not change the fact that the estimated rotation rate is a low limit, because the activity of the inhibitor, which can not be determined easily, is most probably less than 100%. In addition, it is also very likely that not all enzymes are active in the preparations, and we don't know whether the inhibitor binds to otherwise already inactive V-ATPases. Since we assumed 100% activities, for both the inhibitor and the enzyme, smaller activities would scale up the estimated rotation rate. For instance, assuming that the activities of the inhibitor and the enzyme were both 80% (and the inhibitor only binds to the active enzyme), this would mean ~14.89 Hz average rotation rate, instead of ~9.53 Hz, i.e., a factor of 0.8^{-2} larger, for the very same data. Obviously, these uncertainties cause larger errors in the estimation of the rotation rate than those in the titration experiment. Although our approach allows us to report the so far most accurate estimate of the rotation rate in a native V-ATPase in its native membrane environment, it should be concluded that there is still a great demand for an even more accurate measurement that is independent of the chemistry of any inhibitor binding to the enzyme.

Acknowledgment

We thank Ferhan Ayaydin (Cellular Imaging Laboratory, Biological Research Centre Szeged, Hungary) for his help in taking the transmitted light microscopy images of yeast vacuoles. We also thank E. Kónya for excellent technical assistance. Financial support was received from the Hungarian National Science Fund (OTKA K68804 and K101633).

Figures

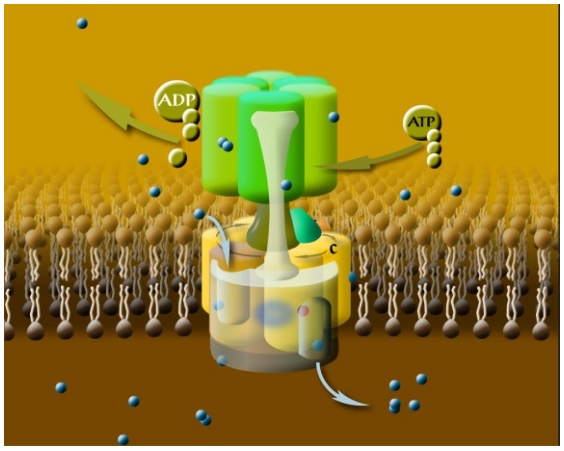

Figure 1. A membrane-bound molecular rotary engine, the vacuolar proton-ATPase (V-ATPase). The subunits of the water-soluble V_1 domain are shown in green, whereas those of the membrane-bound V_o domain are shown in orange-grey colours. For better visibility, subunit a is transparent, not all subunits of the two domains are shown, and the c, c' and c'' subunits are not discriminated. Missing are the the d and e subunits of V_o and the C, E, G, and H subunits of V_1. Binding and hydrolysis of one ATP molecule drives 120 degrees rotation of the rotor (consisting of the "c ring" of a hexameric assembly of subunits c (4 copies), c' and c'' and the d subunits of the Vo domain plus D, F of the V_1 domain) with respect to the stator, driving the transport of two protons from the cytoplasmic side to either intracellular compartments or to the lumen, depending one the location of the V-ATPase, via the hydrophilic input and output channels (or sacks) formed between subunit a and the c ring.

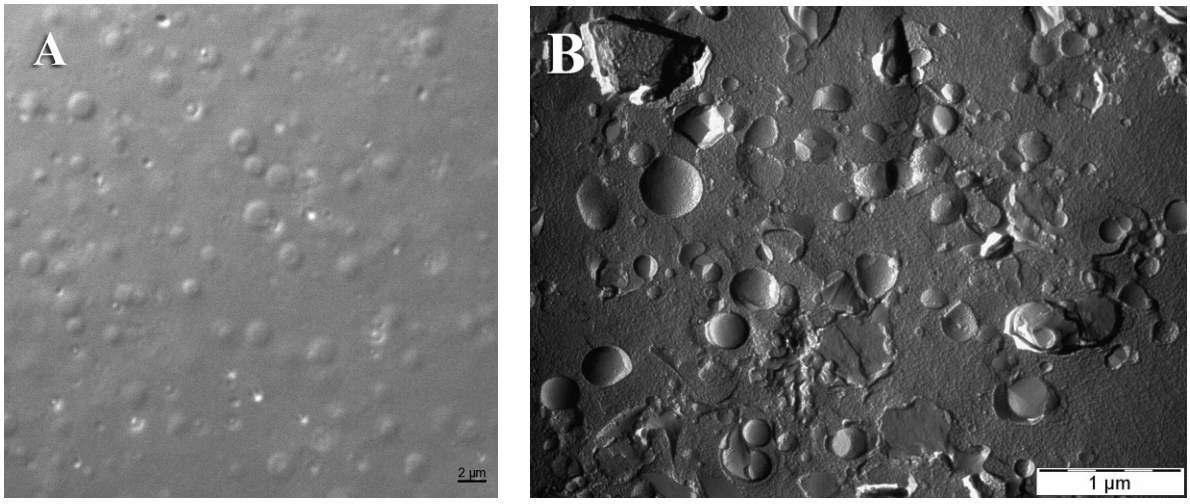

Figure 2. (A) Bright field transmitted light microscopy image of intact vacuoles purified from yeast Saccharomyces cerevisiae. The image was taken with differential interference contrast optics. Scale-bar: 2 µm. (B) Freeze-fracture electron microscopic image of yeast vacuolar vesicles formed from yeast vacuoles after osmotic destruction and washing. The vesicles were fixed in glycerol. Scale-bar: 1 µm.

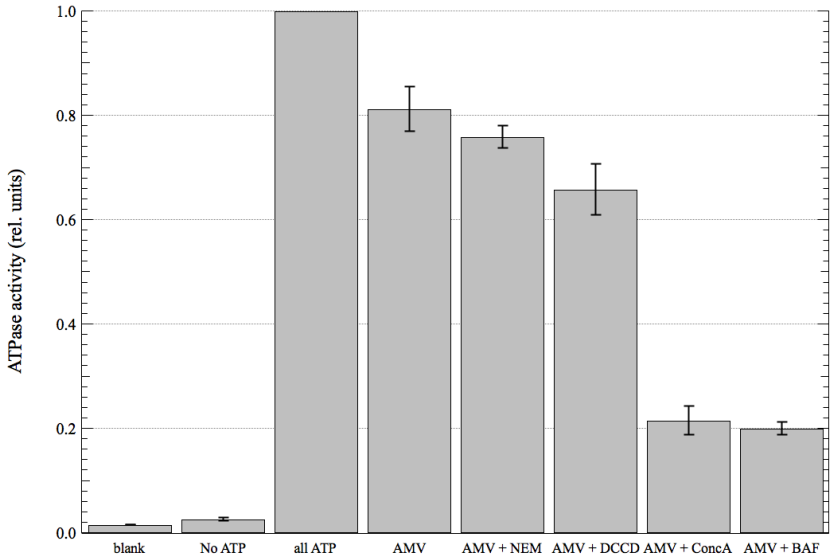

Figure 3. Comparison of ATPase activities of yeast vacuolar vesicles in the presence and absence of different ATPase inhibitors. ATP hydrolysis was stopped after 20 min of incubation at 30 °C in the presence of 2 mM Na_2ATP and 5 mM $MgCl_2$ (except for the first two bars), and the medium was assayed for inorganic phosphate, in all cases. Abbreviations: blank, no vesicles, no ATP, no inhibitor; No ATP, no Na_2ATP, no inhibitor; all ATP, no inhibitors; AMV, 5 mM Na-azide + 0.2 mM molybdenate + 0.1 mM vanadate; AMV + NEM, as AMV plus 2 µM

n-ethyl-maleimide; AMV + DCCD, as AMV plus 2 µM di-cyclohexyl-carbodiimide; AMV + ConcA, as AMV plus 1 µM concanamycin A; AMV + BAF, as AMV plus 1 µM bafilomycin. Results were normalised to the same "all ATP" activity. Bars indicate averages, errors mean a range of ± standard deviation (n = 3).

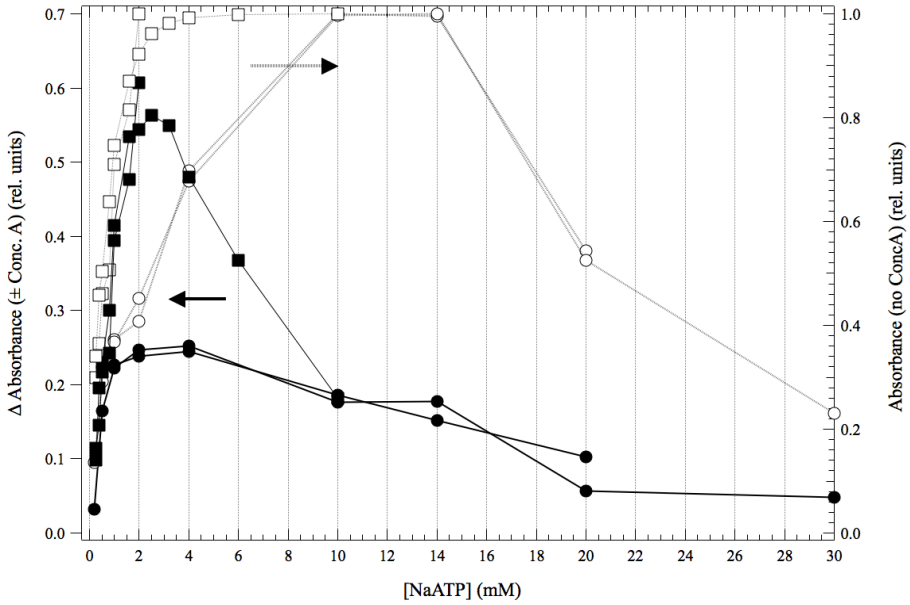

Figure 4. Relative absorbance (at 750 nm) of inorganic phosphate (P_i) liberated by ATP hydrolysis in yeast vacuolar vesicles, and assayed after 20 min incubation at 30 °C, as a function of the concentration of exogenously added Na_2ATP (open symbols, right y-axis). The data were normalised to the same maximum absorbance. Delta absorbance obtained as the difference between the above normalised absorbances in the absence and presence of 1 µM of the specific V-ATPase inhibitor concanamycin A (black symbols, left y-axis). $MgCl_2$ concentration was either kept constant at 5 mM (circles) or was set to 2-fold of the Na_2ATP concentration (squares). Each dataset, at constant or varying concentration of $MgCl_2$, was measured twice from independent cell cultures.

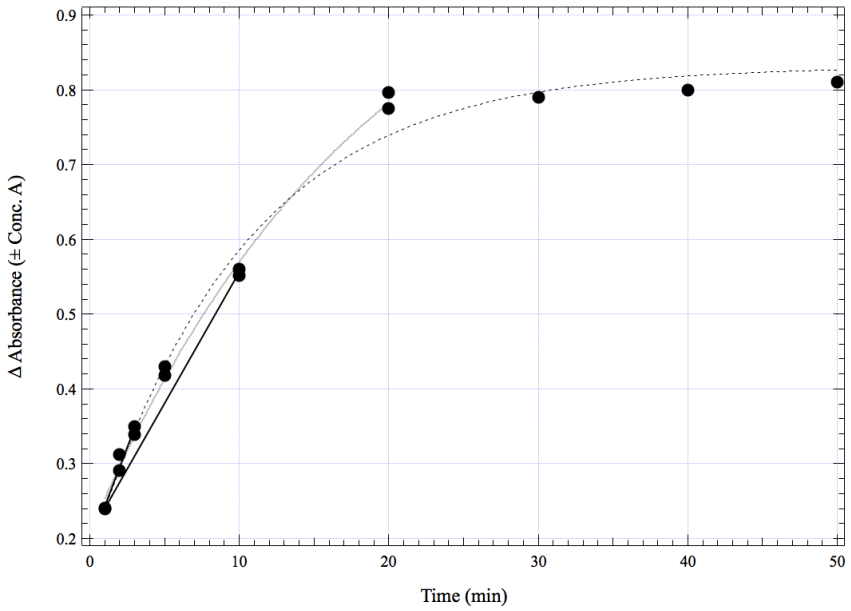

Figure 5. Delta absorbances obtained as the difference between the absorbances (at 750 nm) of assayed inorganic phosphate (P_i) liberated by ATP hydrolysis by yeast vacuolar vesicles in the absence and presence of 1 μM of the specific V-ATPase inhibitor concanamycin A, as a function of the time of incubation at 20 °C and in the presence of exogenously added 2 mM Na_2ATP and 5 mM $MgCl_2$. The dotted and dashed lines are single exponential fits over the 0-10 min and 0-50 min regions, respectively, and are shown just as guides for the eye. The solid line above the 1-3 min time interval is a linear fit to the first 5 points. The solid line over the 0-10 time interval connects the means of the two data points at 1 and 10 min. Over the first 1-20 min region, absorbances were measured twice from independent cell cultures.

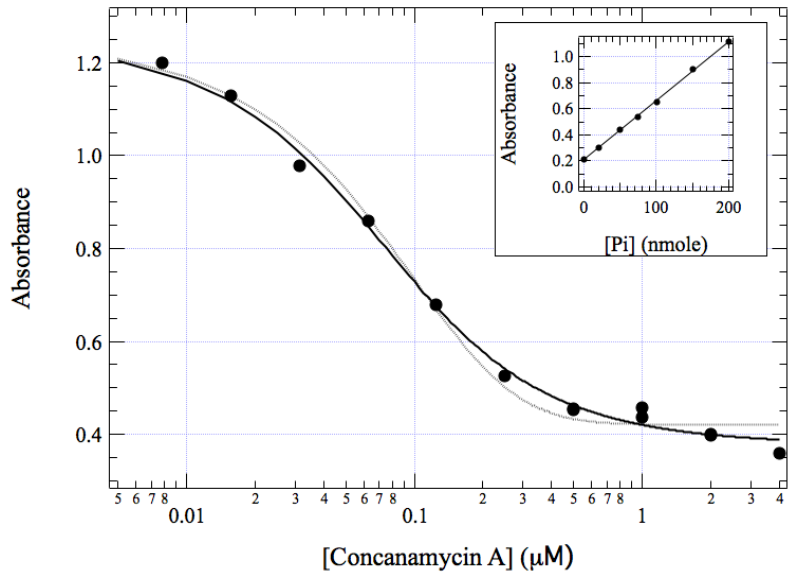

Figure 6. The absorbance (at 750 nm) of inorganic phosphate (P_i) liberated by ATP hydrolysis by yeast vacuolar vesicles, as assayed after 10 min incubation at 20 °C in the presence of 2 mM Na_2ATP (and 5 mM $MgCl_2$), as a function of the concentration of the specific V-ATPase inhibitor, concanamycin A. Three points at zero inhibitor are invisible because of the logarithmic axis. The solid curve is a released fit according to the quadratic binding equation assuming a single binding site per monomeric enzyme (Eq. [6]). The dotted curve is a fit according to the model with 5 binding sites per monomer V-ATPase enzyme (Eq. [9]), but with an enzyme concentration fixed at 44.9 nM. The inset shows the corresponding photometric calibration of absorbance versus the molarity of exogenously added inorganic phosphate [P_i], in the same preparations, same reaction volume and under the same conditions as the titration with the inhibitor, except that no Na_2ATP was added.

References

Adachi K, Oiwa K, Nishizaka T et al. (2007) Coupling of rotation and catalysis in F-1-ATPase revealed by single-molecule imaging and manipulation. Cell 130:309-321

Baars TL, Petri S, Peters C, Mayer A (2007) Role of the V-ATPase in regulation of the vacuolar fission-fusion equilibrium. Mol Biol Cell 18:3873-3882

Beyenbach KW, Wieczorek H (2006) The V-type H+ ATPase: molecular structure and function, physiological roles and regulation. J Exp Biol 209:577-589

Bohrmann J, Bonafede A (2001) Tissue-specific distribution and variation of the channel-forming protein ductin during development of Drosophila melanogaster (vol 44, pg 884, 2000). Int J Dev Biol 45:U4-+

Bowman BJ, McCall ME, Baertsch R, Bowman EJ (2006) A model for the proteolipid ring and bafilomycin/concanamycin-binding site in the vacuolar ATPase of Neurospora crassa. J Biol Chem 281:31885-31893

Bowman EJ, Bowman BJ (2005) V-ATPases as drug targets. J Bioenerg Biomembr 37:431-435

Bowman E, Siebers A, Altendorf K (1988) Bafilomycins - A Class of Inhibitors of Membrane ATPases from Microorganisms, Animal-cells, and Plant-cells. P Natl Acad Sci Usa 85:7972-7976

Cipriano DJ, Wang Y, Bond S et al. (2008) Structure and regulation of the vacuolar ATPases. Bba-bioenergetics 1777:599-604

Clelland ES, Saleuddin AS (2000) Vacuolar-type ATPase in the accessory boring organ of Nucella lamellosa (Gmelin) (Mollusca : Gastropoda): role in shell penetration. Biol Bull 198:272-283

De la Cruz EM, Sweeney HL, Ostap EM (2000) ADP inhibition of myosin V ATPase activity. Biophys J 79:1524-1529

Dixon N, Pali T, Ball S et al. (2003) New biophysical probes for structure-activity analyses of vacuolar-H+-ATPase enzymes. Org Biomol Chem 1:4361-4363

Dixon N, Pali T, Kee TP et al. (2008) Interaction of spin-labeled inhibitors of the vacuolar H+-ATPase with the transmembrane Vo-sector. Biophys J 94:506-514

Dixon N, Pali T, Kee TP, Marsh D (2004) Spin-labelled vacuolar-ATPase inhibitors in lipid membranes. Biochimica et Biophysica Acta - Biomembranes 1665:177-183

Dmitriev OY, Jones PC, Fillingame RH (1999) Structure of the subunit c oligomer in the F1F0 ATP synthase: model derived from solution structure of the monomer and cross-linking in the native ensyme. Proc Natl Acad Sci USA 96:7785-7790

Drose S, Bindseil KU, Bowman EJ, Siebers A, Zeeck A, Altendorf K (1993) Inhibitory Effect of Modified Bafilomycins and Concanamycins on P-Type and V-Type Adenosine-Triphosphatases. Biochemistry-us 32:3902-3906

Dunlop J, Jones PC, Finbow ME (1995) Membrane Insertion and Assembly of Ductin - A Polytopic Channel with Dual Orientations. EMBO J 14:3609-3616

El Far O, Seagar M (2011) A role for V-ATPase subunits in synaptic vesicle fusion? J Neurochem 117:603-612

Farina C, Gagliardi S (1999) Selective inhibitors of the osteoclast vacuolar proton ATPase as novel bone antiresorptive agents {$[$}Review{$]$}. Drug Discovery Today 4:163-172

Feniouk BA, Suzuki T, Yoshida M (2007) Regulatory interplay between proton motive force, ADP, phosphate, and subunit epsilon in bacterial ATP synthase. J Biol Chem 282:764-772

Ferguson SJ (2000) ATP synthase: What dictates the size of a ring? Curr Biol 10:R804-R808

Fillingame RH, Jiang W, Dmitriev OY (2000) Coupling H+ transport to rotary catalysis in F-type ATP synthases: Structure and organization of the transmembrane rotary motor. J Exp Biol 203:9-17

Finbow ME, Harrison MA (1997) The vacuolar H+-ATPase: a universal proton pump of eukaryotes. Biochem J 324:697-712

Finbow ME, John S, Kam E, Apps DK, Pitts JD (1993) Disposition and orientation of ductin (DCCD-Reactive Vacuolar H+-ATPase Subunit) in mammalian membrane complexes. Exp Cell Res 207:261-270

Finbow M, Goodwin SF, Meagher L et al. (1994) Evidence that the 16-Kda Proteolipid (Subunit-c) of the Vacuolar H+-Atpase and Ductin from Gap-Junctions are the Same Polypeptide in Drosophila and Manduca - Molecular-Cloning of the Vha16K Gene from Drosophila. J Cell Sci 107:1817-1824

Finbow ME, Harrison M, Jones P (1995) Ductin - A Proton Pump Component, a Gap Junction Channel and a Neurotransmitter Release Channel. BioEssays 17:247-255

Furuike S, Nakano M, Adachi K, Noji H, Kinosita K, Yokoyama K (2011) Resolving stepping rotation in Thermus thermophilus H+-ATPase/synthase with an essentially drag-free probe. Nat Commun 2:ARTN 233

Futai M, Omote H, Sambongi Y, Wada Y (2000) Synthase (H+ ATPase): coupling between catalysis, mechanical work, and proton translocation. Bba-bioenergetics 1458:276-288

Gagliardi S, Rees M, Farina C (1999) Chemistry and structure activity relationships of bafilomycin A(1), a potent and selective inhibitor of the vacuolar H+-ATPase. Curr Med Chem 6:1197-1212

Gibson LCD, Cadwallader G, Finbow ME (2002) Evidence that there are two copies of subunit c " in V-0 complexes in the vacuolar H+-ATPase. Biochem J 366:911-919

Grabe M, Wang HY, Oster G (2000) The mechanochemistry of V-ATPase proton pumps. Biophys J 78:2798-2813

Hermolin J, Fillingame RH (1989) H+-ATPase activity of Escherichia coli F1F0 is blocked after reaction of dicyclohexylcarbodiimide with a single proteolipid (subunit c) of the F0 complex. J Biol Chem 264:3896-3903

Hinton A, Sennoune SR, Bond S et al. (2009) Function of a Subunit Isoforms of the V-ATPase in pH Homeostasis and in Vitro Invasion of MDA-MB231 Human Breast Cancer Cells. J Biol Chem 284:16400-16408

Hirata R, Graham LA, Takatsuki A, Stevens TH, Anraku Y (1997) VMA11 and VMA16 encode second and third proteolipid subunits of the Saccharomyces cerevisiae vacuolar membrane H+-ATPase. J Biol Chem 272:4795-4803

Hirata T, Iwamoto-Kihara A, Sun-Wada GH, Okajima T, Wada Y, Futai M (2003) Subunit rotation of vacuolar-type proton pumping ATPase - Relative rotation of the G and c subunits. J Biol Chem 278:23714-23719

Holzenburg A, Jones PC, Franklin T et al. (1993) Evidence for a common structure for a class of membrane channels. Eur J Biochem 213:21-30

Huss M, Ingenhorst G, Konig S et al. (2002) Concanamycin a, the specific inhibitor of V-ATPases, binds to the V-o subunit c. J Biol Chem 277:40544-40548

Imamura H, Takeda M, Funamoto S, Shimabukuro K, Yoshida M, Yokoyama K (2005) Rotation scheme of V-1-motor is different from that of F-1-motor. P Natl Acad Sci Usa 102:17929-17933

Itoh H, Takahashi A, Adachi K et al. (2004) Mechanically driven ATP synthesis by F-1-ATPase. Nature 427:465-468

Jefferies KC, Cipriano DJ, Forgac M (2008) Function, structure and regulation of the vacuolar (H+)-ATPases. Arch Biochem Biophys 476:33-42

Kawasaki-Nishi S, Bowers K, Nishi T, Forgac M, Stevens TH (2001) The amino-terminal domain of the vacuolar proton-translocating ATPase a subunit controls targeting and in vivo

dissociation, and the carboxyl-terminal domain affects coupling of proton transport and ATP hydrolysis. J Biol Chem 276:47411-47420

Kawasaki-Nishi S, Nish T, Forgac M (2001) Arg-735 of the 100-kDa subunit a of the yeast V-ATPase is essential for proton translocation. Proc Natl Acad Sci USA 98:12397-12402

Kohori A, Chiwata R, Hossain MD et al. (2011) Torque Generation in F-1-ATPase Devoid of the Entire Amino-Terminal Helix of the Rotor That Fills Half of the Stator Orifice. Biophys J 101:188-195

Kopecky J, Dedina J, Votruba J et al. (1982) Stoicheiometry of dicyclohexylcarbodiimide-ATPase interaction in mitochondria. Biochim Biophys Acta 680:80-87

Kopecky J, Glaser E, Norling B, Ernster L (1981) Relationship between the binding of dicyclohexylcarbodiimide and the inhibition of H+-translocation in submitochondrial particles. FEBS Lett 131:208-212

Kopecky J, Guerrieri F, Papa S (1983) Interaction of dicyclohexylcarbodiimide with the proton-conducting pathway of mitochondrial H+-ATPase. Eur J Biochem 131:17-24

Kota Z, Pali T, Dixon N et al. (2008) Incorporation of transmembrane peptides from the vacuolar H(+)-ATPase in phospholipid membranes: spin-label electron paramagnetic resonance and polarized infrared spectroscopy. Biochemistry 47:3937-3949

Linnett PE, Beechey RB (1979) Inhibitors of the ATP synthethase system. Methods Enzymol 55:472-518

Lowry OH, Rosebrough NJ, Farr L, Randall RJ (1951) Protein measurement with the Folin phenol reagent. J Biol Chem 193:265-275

Lu YD, Qin WX, Li JJ et al. (2005) The growth and metastasis of human hepatocellular carcinoma xenografts are inhibited by small interfering RNA targeting to the subunit ATP6L of proton pump. Cancer Res 65:6843-6849

Lunde CS, Kubo I (2000) Effect of polygodial on the mitochondrial ATPase of Saccharomyces cerevisiae. Antimicrob Agents Chemother 44:1943-1953

Masaike T, Mitome N, Noji H et al. (2000) Rotation of F-1-ATPase and the hinge residues of the beta subunit. J Exp Biol 203:1-8

McHenry P, Wang WLW, Devitt E et al. (2010) Iejimalides A and B Inhibit Lysosomal Vacuolar H+-ATPase (V-ATPase) Activity and Induce S-Phase Arrest and Apoptosis in MCF-7 Cells. J Cell Biochem 109:634-642

Morimura T, Fujita K, Akita M, Nagashima M, Satomi A (2008) The proton pump inhibitor inhibits cell growth and induces apoptosis in human hepatoblastoma. Pediatr Surg Int 24:1087-1094

Nakanishi-Matsui M, Kashiwagi S, Hosokawa H et al. (2006) Stochastic high-speed rotation of Escherichia coli ATP synthase F-1 sector - The epsilon subunit-sensitive rotation. J Biol Chem 281:4126-4131

Nakanishi-Matsui M, Sekiya M, Nakamoto RK, Futai M (2010) The mechanism of rotating proton pumping ATPases. Bba-bioenergetics 1797:1343-1352

Nakano M, Imamura H, Toei M, Tamakoshi M, Yoshida M, Yokoyama K (2008) ATP hydrolysis and synthesis of a rotary motor V-ATPase from Thermus thermophilus. J Biol Chem 283:20789-20796

Nishi T, Forgac M (2002) The vacuolar (H+)-ATPases—Ñnature's most versatile proton pumps. Nature reviews molecular cell biology 3:94-103

Nishio K, Iwamoto-Kihara A, Yamamoto A, Wada Y, Futai M (2002) Subunit rotation of ATP synthase embedded in membranes: a or beta subunit rotation relative to the c subunit ring. P Natl Acad Sci Usa 99:13448-13452

Nishisho T, Hata K, Nakanishi M et al. (2011) The a3 Isoform Vacuolar Type H+-ATPase Promotes Distant Metastasis in the Mouse B16 Melanoma Cells. Mol Cancer Res 9:845-855

Noji H, Yasuda R, Yoshida M, Kinosita K (1997) Direct observation of the rotation of F-1-ATPase. Nature 386:299-302

Ohsumi Y, Uchida E, Anraku Y (1983) Proton-translocating adenosine-triphosphatase in vacuolar membranes of Saccharomyces-cerevisiae. Cell Struct Funct 8:466-466

Okuno D, Iino R, Noji H (2011) Rotation and structure of FoF1-ATP synthase. J Biochem 149:655-664

Otero-Rey EM, Somoza-Martin M, Barros-Angueira F, Garcia-Garcia A (2008) Intracellular pH regulation in oral squamous cell carcinoma is mediated by increased V-ATPase activity via over-expression of the ATP6V1C1 gene. Oral Oncol 44:193-199

Padilla-Lopez S, Pearce DA (2006) Saccharomyces cerevisiae lacking Btn1p modulate vacuolar ATPase activity to regulate pH imbalance in the vacuole. J Biol Chem 281:10273-10280

Pali T, Dixon N, Kee TP, Marsh D (2004) Incorporation of the V-ATPase inhibitors concanamycin and indole pentadiene in lipid membranes. Spin-label EPR studies. Bba-biomembranes 1663:14-18

Pali T, Finbow ME, Holzenburg A, Findlay JBC, Marsh D (1995) Lipid-Protein Interactions and Assembly of the 16-kDa Channel Polypeptide from Nephrops norvegicus. Studies with Spin-Label Electron Spin Resonance Spectroscopy and Electron Microscopy. Biochemistry 34:9211-9218

Pali T, Finbow ME, Marsh D (1997) Membrane assembly of the 16-kDa V-ATPase proteolipid subunit from spin-lattice relaxation enhancements in spin label ESR. Biophys J 72:TUAM7

Pali T, Finbow ME, Marsh D (1999) Membrane assembly of the 16-kDa proteolipid channel from Nephrops norvegicus studied by relaxation enhancements in spin-label ESR. Biochemistry 38:14311-14319

Pali T, Finbow ME, Marsh D (2006) A divalent-ion binding site on the 16-kDa proton channel from Nephrops norvegicus-revealed by EPR spectroscopy. Biochimica et Biophysica Acta - Biomembranes 1758:206-212

Pali T, Whyteside G, Dixon N et al. (2004) Interaction of inhibitors of the vacuolar H+-ATPase with the transmembrane V-o-sector. Biochemistry-us 43:12297-12305

Panke O, Rumberg B (1997) Energy and entropy balance of ATP synthesis. Bba-bioenergetics 1322:183-194

Perez-Sayans M, Somoza-Martin JM, Barros-Angueira F, Rey JMG, Garcia-Garcia A (2009) V-ATPase inhibitors and implication in cancer treatment. Cancer Treat Rev 35:707-713

Powell B, Graham LA, Stevens TH (2000) Molecular characterization of the yeast vacuolar H+-ATPase proton pore. J Biol Chem 275:23654-23660

Rondelez Y, Tresset G, Nakashima T et al. (2005) Highly coupled ATP synthesis by F-1-ATPase single molecules. Nature 433:773-777

Saito T, Schlegel R, Andresson T, Yuge L, Yamamoto M, Yamasaki H (1998) Induction of cell transformation by mutated 16K vacuolar H+-ATPase (ductin) is accompanied by down-regulation of gap junctional intercellular communication and translocation of connexin 43 in NIH3T3 cells. Oncogene 17:1673-1680

Sandermann H (1982) Lipid-dependent Membrane Enzymes - A Kinetic-Model for Cooperative Activation in the Absence of Cooperativity in Lipid-Binding. Eur J Biochem 127:123-128

Seelert H, Poetsch A, Dencher NA, Engel A, Stahlberg H, Muller DJ (2000) Structural biology - Proton-powered turbine of a plant motor. Nature 405:418-419

Sekiya M, Hosokawa H, Nakanishi-Matsui M, Al-Shawi MK, Nakamoto RK, Futai M (2010) Single Molecule Behavior of Inhibited and Active States of Escherichia coli ATP Synthase F-1 Rotation. J Biol Chem 285:42058-42067

Sekiya M, Nakamoto RK, Al-Shawi MK, Nakanishi-Matsui M, Futai M (2009) Temperature Dependence of Single Molecule Rotation of the Escherichia coli ATP Synthase F-1 Sector Reveals the Importance of gamma-beta Subunit Interactions in the Catalytic Dwell. J Biol Chem 284:22401-22410

Serrano R (1978) Characterization of the plasma membrane ATPase of Saccharomyces cerevisiae. Mol Cell Biochem 22:51-63

Stahlberg H, Muller DJ, Suda K et al. (2001) Bacterial Na+-ATP synthase has an undecameric rotor. Embo Rep 2:229-233

Stock D, Leslie AGW, Walker JE (1999) Molecular architecture of the rotary motor in ATP synthase. Science 286:1700-1705

Strasser B, Iwaszkiewicz J, Michielin O, Mayer A (2011) The V-ATPase proteolipid cylinder promotes the lipid-mixing stage of SNARE-dependent fusion of yeast vacuoles. EMBO J 30:4126-4141

Supino R, Petrangolini G, Pratesi G et al. (2008) Antimetastatic effect of a small-molecule vacuolar H+-ATPase inhibitor in in vitro and in vivo preclinical studies. J Pharmacol Exp Ther 324:15-22

Takeda M, Suno-Ikeda C, Shimabukuro K, Yoshida M, Yokoyama K (2009) Mechanism of Inhibition of the V-Type Molecular Motor by Tributyltin Chloride. Biophys J 96:1210-1217

Tsunoda SP, Aggeler R, Yoshida M, Capaldi RA (2001) Rotation of the c subunit oligomer in fully functional F1Fo ATP synthase. Proc Natl Acad Sci U S A 98:898-902

Ubbink-Kok T, Boekema EJ, van Breemen JF, Brisson A, Konings WN, Lolkema JS (2000) Stator structure and subunit composition of the V(1)/V(0) Na(+)-ATPase of the thermophilic bacterium Caloramator fervidus. J Mol Biol 296:311-321

Uchida E, Ohsumi Y, Anraku Y (1985) Purification and properties of H+-translocating, Mg-2+-adenosine triphosphatase from vacuolar membranes of Sacharomyces cerevisiae. J Biol Chem 260:1090-1095

Ueno H, Suzuki T, Kinosita K, Yoshida M (2005) ATP-driven stepwise rotation of FOF1,-ATP synthase. P Natl Acad Sci Usa 102:1333-1338

Van Walraven HS, Strotmann H, Schwarz O, Rumberg B (1996) The H+/ATP coupling ratio of the ATP synthase from thiol-modulated chloroplasts and two cyanobacterial strains is four. FEBS Lett 379:309-313

Wada Y, Sambongi Y, Futai M (2000) Biological nano motor, ATP synthase FoF1: from catalysis to gamma epsilon c(10-12) subunit assembly rotation. Bba-bioenergetics 1459:499-505

Wang YR, Inoue T, Forgac M (2004) TM2 but not TM4 of subunit c " interacts with TM7 of subunit a of the yeast V-ATPase as defined by disulfide-mediated cross-linking. J Biol Chem 279:44628-44638

Whyteside G, Meek PJ, Ball SK et al. (2005) Concanamycin and indolyl pentadieneamide inhibitors of the vacuolar H+-ATPase bind with high affinity to the purified proteolipid subunit of the membrane domain. Biochemistry-us 44:15024-15031

Wilkens S, Vasilyeva E, Forgac M (1999) Structure of the vacuolar ATPase by electron microscopy. J Biol Chem 274:31804-31810

Xie P (2009) On chemomechanical coupling of the F(1)-ATPase molecular motor. Biochim Biophys Acta 1787:955-962

Yasuda R, Noji H, Kinosita K, Motojima F, Yoshida M (1997) Rotation of the gamma subunit in F-1-ATPase; Evidence that ATP synthase is a rotary motor enzyme. J Bioenerg Biomembr 29:207-209

Yasuda R, Noji H, Yoshida M, Kinosita K, Itoh H (2001) Resolution of distinct rotational substeps by submillisecond kinetic analysis of F-1-ATPase. Nature 410:898-904

Yoshida M, Muneyuki E, Hisabori T (2001) ATP synthase - A marvellous rotary engine of the cell. Nat Rev Mol Cell Bio 2:669-677